

# A Stabilized and Coupled Meshfree/Meshbased Method for the Incompressible Navier-Stokes Equations — Part I: Stabilization

Thomas-Peter Fries, Hermann G. Matthies  
Institute of Scientific Computing  
Technical University Braunschweig  
Brunswick, Germany

Informatikbericht Nr.: 2005-02

February, 2005



# A Stabilized and Coupled Meshfree/Meshbased Method for the Incompressible Navier-Stokes Equations — Part I: Stabilization

Thomas-Peter Fries, Hermann G. Matthies  
Department of Mathematics and Computer Science  
Technical University Braunschweig  
Brunswick, Germany

February, 2005

## Location

Institute of Scientific Computing  
Technical University Braunschweig  
Hans-Sommer-Strasse 65  
D-38106 Braunschweig

## Postal Address

Institut für Wissenschaftliches Rechnen  
Technische Universität Braunschweig  
D-38092 Braunschweig  
Germany

## Contact

Phone: +49-(0)531-391-3000  
Fax: +49-(0)531-391-3003  
E-Mail: [wire@tu-bs.de](mailto:wire@tu-bs.de)  
www: <http://www.tu-bs.de/institute/WiR>

**Copyright** © by Institut für Wissenschaftliches Rechnen, Technische Universität Braunschweig

This work is subject to copyright. All rights are reserved, whether the whole or part of the material is concerned, specifically the rights of translation, reprinting, reuse of illustrations, recitation, broadcasting, reproduction on microfilm or in any other way, and storage in data banks. Duplication of this publication or parts thereof is permitted in connection with reviews or scholarly analysis. Permission for use must always be obtained from the copyright holder.

Alle Rechte vorbehalten, auch das des auszugsweisen Nachdrucks, der auszugsweisen oder vollständigen Wiedergabe (Photographie, Mikroskopie), der Speicherung in Datenverarbeitungsanlagen und das der Übersetzung.

# A Stabilized and Coupled Meshfree/Meshbased Method for the Incompressible Navier-Stokes Equations — Part I: Stabilization

Thomas-Peter Fries, Hermann G. Matthies

February, 2005

## Abstract

A stabilized meshfree Galerkin method is employed for the approximation of the incompressible Navier-Stokes equations in Eulerian or arbitrary Lagrangian-Eulerian (ALE) formulation. Equal-order interpolations for velocities and pressure are used. It is well-known from the meshbased context, i.e. from finite volume and finite element methods, that in convection-dominated flow problems in Eulerian or ALE formulation, stabilization is a crucial requirement for reliable solutions. Also, stabilization is needed in order to enable equal-order interpolations of the incompressible Navier-Stokes equations. Standard stabilization techniques, developed in a meshbased context, are extended to meshfree methods. It is found that the same structure of the stabilization schemes may be used, however the aspect of the stabilization parameter, weighing the stabilization terms, has to be reconsidered. In part II of this work, the resulting stabilized meshfree Galerkin method is coupled with a stabilized finite element method. The resulting coupled method employs the comparatively costly meshfree Galerkin method only where it is needed—i.e. in areas of the domain, where a mesh is difficult to maintain—, and the efficient meshbased finite element method is used in the rest of the domain. The fluid solver resulting from this technique is able to solve complex flow problems, involving large deformations of the physical domain and/or moving and rotating obstacles.

# Contents

<b>1</b>	<b>Introduction</b>	<b>3</b>
<b>2</b>	<b>Meshfree Methods</b>	<b>5</b>
<b>3</b>	<b>Governing Equations</b>	<b>6</b>
<b>4</b>	<b>Stabilization</b>	<b>7</b>
4.1	Convection-dominated Problems . . . . .	8
4.2	The Babuška-Brezzi Condition . . . . .	9
4.3	Stabilized Incompressible Navier-Stokes Equations . . . . .	11
<b>5</b>	<b>The Stabilization Parameter</b>	<b>11</b>
5.1	Standard Formulas for $\tau$ . . . . .	12
5.2	One-Dimensional Advection-Diffusion Equation . . . . .	14
5.3	Linear FEM . . . . .	15
5.4	Meshfree Methods . . . . .	16
5.5	Small Dilatation Parameters . . . . .	17
5.6	Stabilization Parameter in Multi-Dimensions . . . . .	18
<b>6</b>	<b>Numerical Results</b>	<b>19</b>
6.1	One-dimensional Advection-Diffusion Equation . . . . .	20
6.2	Incompressible Navier-Stokes Equations . . . . .	21
6.2.1	Driven Cavity Flow . . . . .	21
6.2.2	Flow Past a Cylinder . . . . .	24
<b>7</b>	<b>Conclusion</b>	<b>26</b>
	<b>References</b>	<b>26</b>

# 1 Introduction

The motivation for this work is the simulation of complex fluid and fluid-structure interaction problems. A number of methods have been developed for the numerical simulation of flow problems, each with its characteristic advantages and disadvantages. One may characterize these methods based on the fact whether they employ a mesh for the discretization or not. Meshbased methods may be labeled standard tools in the numerical world. Well-known members of this class are the finite volume method (FVM) and the finite element method (FEM). Both these methods are used frequently and reliably for the approximation of the Navier-Stokes equations [15, 24, 28, 58], the governing equations of fluid dynamics. The success of the approximations depends on the ability to construct and maintain meshes of sufficient quality throughout the whole simulation. This, however, may pose serious problems in complex flow problems, for example in thus involving large deformations of the domain or moving and rotating obstacles.

Recently, a new class of so-called meshfree methods (MMs) has been developed, which approximate partial differential equations based on a set of nodes without the need of an additional mesh. The price to pay for this is the relatively high computational burden often associated with the use of these methods. Rather than calling these methods an alternative for meshbased methods, one may label them specific tools, because they are frequently used in problems where meshes are difficult or impossible to maintain. A large number of meshfree methods have been developed during the last three decades, among them the popular element-free Galerkin (EFG) method [8] and smoothed particle hydrodynamics (SPH) [49]. For an overview of MMs see [7, 19].

The use of MMs for the simulation of challenging real-life problems is often inhibited by the increased computational cost, when compared with a meshbased simulation. This is particularly true for meshfree Galerkin methods, where a time-consuming integration of the weak form under consideration is required. Therefore, MMs for the simulation of flow problems are usually applied in collocation settings, where the strong form of a problem is considered and no integration is needed. Advantages and disadvantages of meshfree collocation and Galerkin methods are well-known, and may be reduced to the statement that for the same number of unknowns Galerkin methods are in general more accurate and robust, but also computationally more demanding than collocation methods, see e.g. [5, 6, 11, 14].

Therefore, it seems promising to couple standard meshbased methods like the FEM with *mesh-free Galerkin methods*. Then, it is possible to use meshfree methods only in small regions of the domain, where a mesh is difficult to maintain, and meshbased standard methods in all other parts. Accuracy and robustness are expected to be favorable and the computational work is expected to scale with the meshbased part, rather than with the meshfree one. The issue of coupling meshfree and meshbased methods for the approximation of the incompressible Navier-Stokes equations is dealt with in part II of this work [22].

Rather than separating numerical methods into meshfree and meshbased, one may consider different formulations of the underlying differential equations. Most importantly Lagrangian, Eulerian, and arbitrary Lagrangian-Eulerian (ALE) formulations [38] have to be considered which choose distinct coordinate systems for the description of the problem. The most important difference in the formulations is in the presence of an advection term in the Eulerian and ALE formulations, which is absent in the Lagrangian description. Advection terms are non-selfadjoint

operators that often lead to problems in their numerical treatment, e.g. [10]. This is particularly the case for Bubnov-Galerkin methods, where the test functions are chosen equal to the shape functions. Spurious oscillations may pollute the overall solution and stabilization is required, see e.g. [10].

Numerical problems (locking, singular matrices etc.) may also occur with so-called mixed problems [18], the incompressible Navier-Stokes equations fall into this class. Applying the same shape functions to all variables of the problems in a Bubnov-Galerkin setting (equal-order interpolation), which is from a computational viewpoint the most convenient way, leads to severe problems as a result from violating certain conditions. Stabilization is a possibility to overcome these problems [18].

The need for stabilization is well studied in the meshbased context, e.g. [10, 15, 37]. A number of stabilization methods have been developed to overcome numerical problems. This stems from the fact that for meshbased methods the Eulerian or ALE formulation is standard, e.g. [15, 28], because it seems impossible to maintain a conforming mesh in most flow problems with the Lagrangian formulation. Then, stabilization is a crucial ingredient to obtain suitable solutions.

*Eulerian and ALE meshfree methods* are not only of interest in their own right, but are a natural choice for the desired coupling of meshbased and meshfree methods. So far, MMs for fluid simulation have usually been used in Lagrangian formulations, i.e. as particle methods [41, 48, 49, 57]. To successfully use Eulerian or ALE meshfree methods in Galerkin settings, the problem of stabilization has to be solved. This is the main aspect of part I of this work. In the following, two standard stabilization schemes known from the meshbased context are applied to the incompressible Navier-Stokes equations: One is the streamline-upwind/Petrov-Galerkin method [10] together with the pressure-stabilizing/Petrov-Galerkin method [55] (SUPG/PSPG), the other is the Galerkin/least-squares method [37] (GLS). Both methods add products of perturbation terms with residual terms of the governing problem to the weak form, weighted with a stabilization parameter  $\tau$  [20]. They stabilize oscillations in convection-dominated regimes, and overcome problems associated with equal-order interpolations in mixed formulations. It is found that SUPG/PSPG as well as GLS stabilization can be applied straightforward to meshbased and meshfree problems. However, the aspect of the stabilization parameter  $\tau$  has to be reconsidered: Standard formulas for  $\tau$  are often deduced for linear finite element shape functions. Applications to higher order elements as well as to meshfree shape functions requires special attention [16, 17, 20, 21].

The paper is organized as follows: In section 2 the moving least-squares (MLS) procedure for the construction of meshfree shape functions—as employed in the EFG method—is briefly recalled. These shape functions are later employed in the Petrov-Galerkin weak formulation of the stabilized incompressible Navier-Stokes equations. The governing equations of incompressible flow are shown in section 3. Section 4 discusses the need for stabilization of the incompressible Navier-Stokes equations. Taking the development of stabilized methods in the meshbased context as a guideline, similar steps have been taken in MMs. The state-of-the-art in stabilized MMs is discussed here. In section 5 the aspect of suitable stabilization parameters  $\tau$  is considered. A new generalized approach is shown to obtain formulas for  $\tau$  for arbitrary shape functions that leads to nodally exact solutions for a simple one-dimensional model equation. Standard meshbased formulas for  $\tau$  are recovered if linear finite element shape functions are employed. It is found that the same formulas may only be used in a meshfree context if small dilatation parameters of the

meshfree shape functions are used. This statement is confirmed by the numerical results presented in section 6, where it is also found that SUPG/PSPG stabilized results are slightly less diffusive than GLS stabilized results. The paper ends in section 7 with a short summary and conclusion.

## 2 Meshfree Methods

In this section the chosen meshfree method (MM) for the approximation of the incompressible Navier-Stokes equations is briefly introduced. For a detailed overview of MMs see [7, 19]. Throughout this paper meshfree shape functions are constructed with the moving least-squares (MLS) technique [43], and are used in a Galerkin setting for the approximation of the weak form. This Galerkin method is equivalent to the element-free Galerkin (EFG) method of Belytschko *et al.* [8]. The EFG has originally been applied in Bubnov-Galerkin settings and involves a certain integration technique and treatment of Dirichlet boundary conditions [8]. However, herein, we use the term EFG as a general term for a Galerkin MM for arbitrary Petrov-Galerkin formulations and do not consider the integration, and boundary condition aspects as being a crucial and identifying part of the method.

MLS shape functions are constructed as follows, see e.g. [7, 19, 43]: Consider a domain  $\Omega$  with boundary  $\Gamma$ .  $\Omega$  is discretized by a set of  $n$  nodes (particles)  $I = \{\mathbf{x}_1, \dots, \mathbf{x}_n\}$  with corresponding dilatation parameters  $\rho_i$ , which determine the supports  $\tilde{\Omega}_i \subseteq \Omega$  of the resulting meshfree shape functions. One defines an approximation of a function  $u(\mathbf{x})$  of [43]

$$u(\mathbf{x}) \approx \tilde{u}(\mathbf{x}) = \mathbf{p}^T(\mathbf{x}) \mathbf{a}(\mathbf{x}), \quad (2.1)$$

where  $\mathbf{p}(\mathbf{x})$  forms a basis of the approximation subspace, which generally consists of monomials. The length  $k$  of this vector depends on the dimension of the problem, and the desired order of consistency of the resulting approximations. Throughout this paper first order consistency is assumed, which results in the ability of the meshfree shape functions in weighted residual settings to find linear solutions exactly. The vector  $\mathbf{a}(\mathbf{x})$  is the vector of unknown coefficients of the approximation at  $\mathbf{x}$ . These unknowns are determined by a minimization of the following weighted error functional:

$$\begin{aligned} J(\mathbf{a}) &= \sum_{i \in I} w(\mathbf{x} - \mathbf{x}_i) [u(\mathbf{x}_i) - \tilde{u}(\mathbf{x}_i)]^2, \\ &= \sum_{i \in I} w(\mathbf{x} - \mathbf{x}_i) [\mathbf{u} - \mathbf{p}^T(\mathbf{x}_i) \mathbf{a}(\mathbf{x})]^2, \end{aligned} \quad (2.2)$$

which leads to a  $k \times k$  system of equations for  $\mathbf{a}(\mathbf{x})$ . The weighting function  $w(\mathbf{x} - \mathbf{x}_i)$  is in general a bell-shaped function—e.g. an approximation of the Gaussian function, see [19] for frequent choices of  $w(\mathbf{x} - \mathbf{x}_i)$ —and is non-zero only in the corresponding support  $\tilde{\Omega}_i$ . This ensures the locality of the approximation. The resulting system of equation is

$$\sum_{i \in I} w(\mathbf{x} - \mathbf{x}_i) \mathbf{p}(\mathbf{x}_i) \mathbf{p}^T(\mathbf{x}_i) \mathbf{a}(\mathbf{x}) = \sum_{i \in I} w(\mathbf{x} - \mathbf{x}_i) \mathbf{p}(\mathbf{x}_i) \mathbf{u}, \quad (2.3)$$

$$\mathbf{M}(\mathbf{x}) \mathbf{a}(\mathbf{x}) = \mathbf{B}(\mathbf{x}) \mathbf{u}, \quad (2.4)$$

hence  $\mathbf{a}(\mathbf{x}) = [\mathbf{M}(\mathbf{x})]^{-1} \mathbf{B}(\mathbf{x}) \mathbf{u}$ . In words, the minimization of the error functional enables one to find a connection between the unknown coefficients  $\mathbf{a}(\mathbf{x})$  of the approximation with the nodal unknowns  $\mathbf{u}$ . Inserting  $\mathbf{a}(\mathbf{x})$  into the approximation gives

$$\begin{aligned} \tilde{u}(\mathbf{x}) &= \mathbf{p}^T(\mathbf{x}) [\mathbf{M}(\mathbf{x})]^{-1} \mathbf{B}(\mathbf{x}) \mathbf{u} \\ &= \mathbf{p}^T(\mathbf{x}) [\mathbf{M}(\mathbf{x})]^{-1} \sum_{i \in I} w(\mathbf{x} - \mathbf{x}_i) \mathbf{p}(\mathbf{x}_i) \mathbf{u}, \end{aligned} \quad (2.5)$$

where the meshfree shape functions  $N_i(\mathbf{x}) = \mathbf{p}^T(\mathbf{x}) [\mathbf{M}(\mathbf{x})]^{-1} w(\mathbf{x} - \mathbf{x}_i) \mathbf{p}(\mathbf{x}_i)$  may be directly extracted. Fig. 1 shows a one-dimensional example of meshfree shape functions with first order consistency in a domain  $\Omega = (0, 1)$ , discretized by 11 regularly distributed nodes, and a constant dilatation parameter of  $\rho_i = 3.3\Delta x$ .

The MLS shape functions build a partition of unity (PU) of a certain order [7] in  $\Omega$

$$\sum_{i \in I} N_i(\mathbf{x}) \mathbf{p}(\mathbf{x}_i) = \mathbf{p}(\mathbf{x}) \quad \mathbf{x} \in \Omega, \quad (2.6)$$

and this order depends on the choice of  $\mathbf{p}$ . It is important to note that MLS shape functions lack the Kronecker- $\delta$  property of standard nodal finite element shape functions, that is  $N_i(x_j) \neq \delta_{ij}$ . Furthermore, the MLS shape functions have often of a highly non-polynomial character especially for higher order derivatives. This makes integration in a Galerkin setting demanding, and requires considerably more integration points than for meshbased finite element shape functions. At each integration point summation expressions have to be evaluated, which includes a neighbour search and a matrix inversion ( $[\mathbf{M}(\mathbf{x})]^{-1}$ ). This is done at run-time and defines the connectivity of the nodes. The need to build up and invert small system of equations at large numbers of integration points is the major drawback of MMs, and the integration of the weak form under consideration takes considerably more time than with standard meshbased methods.

In part II of this work [22] meshfree and meshbased methods are coupled, in order to use the computationally more demanding meshfree shape functions only in small parts of  $\Omega$  where a mesh causes severe problems, and efficient standard meshbased finite element shape functions in the rest of the domain. In the sequel of this part, we restrict ourselves to meshfree approximations only, and focus on stabilization aspects.

### 3 Governing Equations

It is our aim to solve the incompressible Navier-Stokes equations in the velocity-pressure formulation. In this part of the paper only the stationary form is considered, in part II the instationary form is solved. Let  $\Omega$  be the spatial domain, then in  $\Omega$

$$\varrho(\mathbf{u} \cdot \nabla \mathbf{u} - \mathbf{f}) - \nabla \cdot \boldsymbol{\sigma} = 0, \quad (3.1)$$

$$\nabla \cdot \mathbf{u} = 0, \quad (3.2)$$

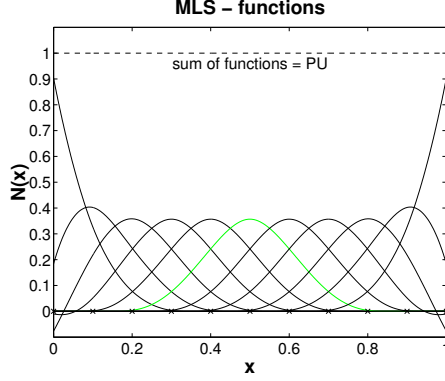


Figure 1: Example of MLS shape function in a one-dimensional domain.

where  $\mathbf{u}$  are the velocities,  $\rho$  is the density.  $\boldsymbol{\sigma}$  is the stress tensor defined as

$$\boldsymbol{\sigma} = -p\mathbf{I} + 2\mu\boldsymbol{\varepsilon}(\mathbf{u}), \text{ with } \boldsymbol{\varepsilon}(\mathbf{u}) = \frac{1}{2} \left( \nabla\mathbf{u} + (\nabla\mathbf{u})^T \right), \quad (3.3)$$

$p$  is the pressure, and  $\mu$  the dynamic viscosity. The Dirichlet and Neumann boundary conditions are applied along complementary subsets of the boundary of  $\Omega$ ,  $\Gamma_{\mathbf{g}}$  and  $\Gamma_{\mathbf{h}}$ , as

$$\mathbf{u} = \mathbf{g} \text{ on } \Gamma_{\mathbf{g}}, \quad (3.4)$$

$$\boldsymbol{\sigma} \cdot \mathbf{n} = \mathbf{h} \text{ on } \Gamma_{\mathbf{h}}. \quad (3.5)$$

For a Galerkin approximation, the test and trial functions for the velocities and pressure are from the sets

$$\mathcal{S}_{\mathbf{u}}^h = \left\{ \mathbf{u}^h \mid \mathbf{u}^h \in (\mathcal{H}^{1h})^{n_d}, \mathbf{u}^h = \mathbf{g}^h \text{ on } \Gamma_{\mathbf{g}} \right\}, \quad (3.6)$$

$$\mathcal{V}_{\mathbf{u}}^h = \left\{ \tilde{\mathbf{w}}^h \mid \tilde{\mathbf{w}}^h \in (\mathcal{H}^{1h})^{n_d}, \tilde{\mathbf{w}}^h = 0 \text{ on } \Gamma_{\mathbf{g}} \right\}, \quad (3.7)$$

$$\mathcal{S}_p^h = \mathcal{V}_p^h = \left\{ q^h \mid q^h \in \mathcal{H}^{1h} \right\}, \quad (3.8)$$

where  $n_d$  is the number of space dimensions and  $\mathcal{H}^{1h}$  is a finite dimensional space built by the set of shape functions. Then, the weak form of the problem may be stated as: find  $\mathbf{u}^h \in \mathcal{S}_{\mathbf{u}}^h$  and  $p^h \in \mathcal{S}_p^h$  such that

$$\int_{\Omega} \tilde{\mathbf{w}}^h \cdot \rho \left( \frac{\partial \mathbf{u}^h}{\partial t} + \mathbf{u}^h \cdot \nabla \mathbf{u}^h - \mathbf{f}^h \right) + \boldsymbol{\varepsilon}(\tilde{\mathbf{w}}^h) : \boldsymbol{\sigma}^h(\mathbf{u}^h, p^h) d\Omega + \int_{\Omega} q^h \nabla \cdot \mathbf{u}^h d\Omega = \oint_{\Gamma_{\mathbf{h}}} \tilde{\mathbf{w}}^h \cdot \mathbf{h}^h d\Gamma \quad \forall \tilde{\mathbf{w}}^h \in \mathcal{V}_{\mathbf{u}}^h, \forall q^h \in \mathcal{V}_p^h. \quad (3.9)$$

## 4 Stabilization

Using numerical methods in a straightforward way for the approximation of arbitrary differential equations may cause severe problems. Oscillations, locking, singular matrices and other problems may be the result of disregarding important mathematical statements related with a certain

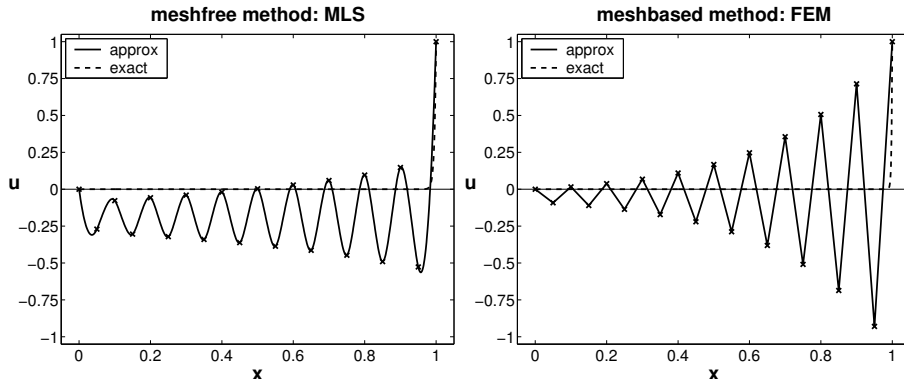


Figure 2: Typical oscillations in the approximation of an advection-dominated problem in one dimension. Standard Bubnov-Galerkin methods are applied, based on meshfree and meshbased shape functions.

concrete problem.

For the incompressible Navier-Stokes equations, stabilization is needed due to the advection term  $\mathbf{u} \cdot \nabla \mathbf{u}$ , and due to the incompressibility constraint  $\nabla \cdot \mathbf{u} = 0$ , which is discussed in the following.

#### 4.1 Convection-dominated Problems

It is well-known that Bubnov-Galerkin weighted residual methods—where test and shape functions span the same space—cause severe oscillations in the overall solution of a convection-dominated problem, see e.g. [10]. This does not only lead to qualitatively bad results, but even violates basic physical principles like entropy or the positivity of concentrations etc. [28]. Fig. 2 shows an oscillatory example for a meshbased and a meshfree Bubnov-Galerkin approximation of the one-dimensional advection-diffusion equation, Eq. (5.8), which is highly advection-dominated. The same phenomenon occurs in the context of central finite differences and finite volumes [27, 28]. The reason for these instabilities can be found in the non-self adjointness of the convective operators [10].

In the seventies, several stabilized FEMs have been proposed, see [13, 26, 32, 40]. These methods often try to incorporate stabilizing upwind effects, which is closely related to introduction of artificial diffusion [10]. However, application of these ideas to general, time-dependent and/or multi-dimensional problems often leads to unsatisfactory over-diffusive approximations, which can be explained by the inconsistency of the stabilized formulations [10]. The streamline-upwind/Petrov-Galerkin (SUPG) method, introduced by Brooks and Hughes in [10] (and [34]) may be considered the first successful stabilization technique to prevent oscillations in convection-dominated problems in the FEM. The main steps are: introduce artificial diffusion in streamline direction only, interpret this as a modification of the test function of the advection terms, and finally, enforce consistency such that this modified test function is applied to *all* terms of the weak form [10, 20]. The resulting SUPG stabilized weak formulation is still consistent, i.e. the exact solution of the problem still satisfies the stabilized equations. An important part of the theoretical analysis of the SUPG has been done by Johnson, see [39, 50] and references therein.

Motivated from mathematical analysis, another type of stabilization scheme has been established, the Galerkin/least-squares (GLS) method [37]. It is similar to the SUPG in certain aspects, and for purely hyperbolic equations and/or linear interpolation functions, the two become identical [37]. In the GLS method, least-squares forms of the residuals are added to the Galerkin method, enhancing the stability of the Bubnov-Galerkin method without giving up consistency [37].

Today, the SUPG and GLS stabilizations are most frequently used to stabilize FEM formulations, see e.g. [15]. Both stabilization methods add products of perturbations and residuals to the weak form, weighted with a so-called stabilization parameter  $\tau$ . The suitable choice of  $\tau$ , leading to reliable oscillation-free approximations, is a crucial aspect in stabilized methods [53].

Recently, stabilization has also been applied to meshfree methods [1, 25, 30, 42, 44, 45, 51, 52]. The same principles as for the FEM stabilizations have been used here. Upwind ideas for meshfree collocation methods—analogously to the meshbased FDM—have been examined e.g. by Kuhnert in [42], a different way is taken by Oñate *et al.* in [51, 52]. For meshfree Galerkin methods, upwind ideas have been investigated e.g. by Atluri *et al.* in [1]. There, the supports of the test functions are shifted in upstream direction depending on the local convection-diffusion ratio.

SUPG and GLS stabilized meshfree Galerkin methods have been successfully applied, e.g. by Huerta *et al.* in [30], by Liu *et al.* in [45] and by Li *et al.* in [44] for the solution of linear advection-diffusion problems. In [25], Günther applies SUPG stabilization to the compressible Navier-Stokes equations. It is not surprising that SUPG and GLS stabilizations work successfully for meshbased *and* meshfree methods as well, because close similarities in the theoretical analysis can be shown, see e.g. [3, 4]. Therefore, one may expect that the theoretical foundation of SUPG and GLS accomplished for the meshbased FEM applies analogously to meshfree methods.

*However, this is not generally true for the stabilization parameter  $\tau$ .* It is shown in section 5 that the resulting formulas for the parameter  $\tau$  are highly dependent on the shape functions of the approximation. The standard formulas for  $\tau$  used in the meshbased FEM context are derived for linear finite element shape functions. Application of these formulas to MMs does in general not lead to suitable results; this is also noted e.g. in [45] and [25]. In section 5 it is shown when standard meshbased formulas for  $\tau$  applied to MMs are suitable.

## 4.2 The Babuška-Brezzi Condition

Variational formulations associated with constraints may lead to severe problems if standard numerical methods are used in a straightforward manner. One way to treat these problems is to use admissible functions satisfying the constraint *ab initio* [18]. The solution is then a member of a smaller space of functions than the space required from continuity conditions alone, and suitable interpolations are not easy to find. Instead, the problem can be reformulated by introducing a second variable, the Lagrange multiplier [18]. The resulting variational formulation falls into an abstract class of "mixed" formulations. Lagrange multipliers and mixed approximations are thus intimately related. The governing stability conditions for mixed problems are the *Babuška-Brezzi condition* and *K*-ellipticity [2, 9]. Violating them leads to pathologies such as spurious oscillations and locking [18], or the resulting system of equations may be singular not giving a unique solution at all.

The incompressible Navier-Stokes equations and its non-advective counterpart, the Stokes

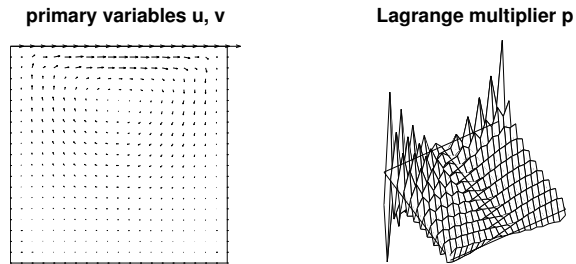


Figure 3: The solution for Stokes flow with P1/P1 FEM and a wrong stabilization parameter  $\tau \approx 0$ . Although the primary variables (velocity field) are reasonably approximated, the Lagrange multiplier (pressure field) shows large oscillations.

equations, fall into this class of mixed methods. Fig. 3 shows an example for Stokes flow with large oscillations in the pressure field as a consequence of violating the Babuška-Brezzi condition. Thus, the approximation of the incompressible Navier-Stokes and Stokes equations requires careful choice of the combination of interpolation functions. In particular, equal-order interpolations, where the same ansatz is made for the primary and secondary (Lagrange multiplier) variables are *not* adequate in a Bubnov-Galerkin setting, although from an implementational viewpoint they are most desirable [55].

Therefore, it is often important to find ways to *circumvent* the Babuška-Brezzi condition rather than finding interpolations fulfilling it [18]. Motivated from theory this can be done by modifying the bi-linear form in a way that it is coercive on the primal variable as well as the Lagrange multiplier. Then, there is no need to fulfill the Babuška-Brezzi condition for this method. This can be interpreted as some kind of stabilization which is realized by adding appropriate perturbation terms, without upsetting consistency. This is realized—with the same fundamental idea as in other stabilizations—by a multiplication of perturbations with residual forms of the governing problem.

Stabilizations of the Stokes equations in the FEM context have been presented in [36], and in [55] for the incompressible Navier-Stokes equations. Both methods are very similar in that they only perturb the test function of the Lagrange multiplier, i.e. the pressure, leading to unsymmetric systems of equations for Stokes flow. This kind of stabilization is called pressure-stabilizing/Petrov-Galerkin (PSPG) throughout this paper, as proposed in [55]. In [35], Stokes flow has been stabilized with GLS stabilization, leading to perturbations of all test functions but maintaining symmetry. Note that GLS was already mentioned in the previous subsection for the stabilization of convection-dominated problems, and can also be used here to circumvent the Babuška-Brezzi condition. This is not the case for SUPG stabilization which is only successful in suppressing oscillations from convection-dominated problems. Thus, in the following GLS stabilization is considered on the one hand, and SUPG/PSPG stabilization on the other.

In a meshfree context the aspects of mixed problems and problems with constraints have been investigated e.g. by Huerta *et al.* in [31], where a pseudo-divergence-free interpolation space is defined, enabling to fulfill the Babuška-Brezzi condition. There it is also pointed out that incompressibility in meshfree methods is still an open question. Related to finite elasticity and locking, the contributions in [12] and [29] are mentioned, the pressure projection method in the former is also known in the FEM context for the incompressible Navier-Stokes and Stokes equations.

Stabilization of these problems in a meshfree context, equivalent to PSPG stabilization, may be found in [44] for Stokes flow.

### 4.3 Stabilized Incompressible Navier-Stokes Equations

According to the previous subsections the incompressible Navier-Stokes equations are approximated in SUPG/PSPG and GLS form. In both cases Petrov-Galerkin formulations result, where the test functions differ from the corresponding shape functions.

The SUPG/PSPG stabilized approximation of the weak form of the incompressible Navier-Stokes equations results from (3.9) with the test functions  $\tilde{\mathbf{w}}^h$  of

$$\tilde{\mathbf{w}}^h = \mathbf{w}^h + \tau_{\text{SUPG}} (\mathbf{u}^h \cdot \nabla) \mathbf{w}^h + \tau_{\text{PSPG}} \frac{1}{\varrho} \nabla q^h, \quad (4.1)$$

where  $\mathbf{w}^h = \mathbf{N}^h$ . The GLS stabilized weak form is (3.9) with the following test functions

$$\tilde{\mathbf{w}}^h = \mathbf{w}^h + \frac{\tau_{\text{GLS}}}{\varrho} [\varrho (\mathbf{u}^h \cdot \nabla) \mathbf{w}^h - \nabla \cdot \boldsymbol{\sigma} (\mathbf{w}^h, q^h)]. \quad (4.2)$$

In practice often  $\tau = \tau_{\text{SUPG}} = \tau_{\text{PSPG}} = \tau_{\text{GLS}}$ , e.g. [10, 37, 53, 55]. It may thus be seen that the two stabilization methods differ in the presence of additional diffusion terms in the GLS method.

**Remark 1** In case of  $C^0$ -continuous finite element shape functions, one has to consider the stabilizing terms over element interiors  $\Omega_e$  only, usually written as  $\sum_{e=1}^{n_{\text{el}}} \int_{\Omega_e}$ , see e.g. [10], because also second order terms occur in the stabilized weak form. This however can be considered as not being fully consistent, and may result in a convergence order degradation in some cases [30]. Least-squares recovering techniques of second derivatives of the shape functions offer help, but the increase in computational cost is not negligible [30]. In contrast, meshfree shape functions can be chosen to have any desired order of continuity, and second derivatives introduced by the stabilizing terms are well defined everywhere in  $\Omega$ .

## 5 The Stabilization Parameter

Each of the stabilization methods described in the previous section consists of two ingredients: The structure of the perturbation and the stabilization parameter  $\tau$ . It can easily be shown that the same arguments for the structure of the stabilization schemes hold both for meshfree and mesh-based methods [30]. However, this is in general not true for the stabilization parameter  $\tau$  itself.

In the finite element context, there are several suggestions for the determination of  $\tau$  in the literature, i.e. with the help of element matrix and vector norms [56], the Green's function of the element [33], mathematical error analysis [16, 17, 37], or model equations [13, 26, 40].

From mathematical analysis in the finite element context, one can find the following design criteria for the stabilization parameter:  $\tau > 0$  in general,  $\tau = O(h^2/\mu)$  for low element Peclet numbers  $\text{Pe} = |\mathbf{c}|h/(2K)$ , and  $\tau = O(h/|\mathbf{c}|)$  for high Peclet numbers, where  $h$  is a measure of the node distribution, and  $\mu$  and  $|\mathbf{c}|$  are measures of the diffusion and convection respectively.

A number of formulas that fulfill these basic requirements for the stabilization parameter are available in the finite element context, see subsection 5.1.

The question of an 'optimal' stabilization parameter  $\tau$  requires an optimality criterion of the resulting approximation. Often the one-dimensional advection-diffusion equation is taken as a model equation. There, the exact solution is known, and enables one to calculate stabilization parameters that fulfill any desired optimality criterion. An optimality criterion that has proven to be particularly useful is the one that obtains *the nodally exact solution* of the model equation. It can be shown that for linear FEM and a regular node distribution, the "coth-formula"

$$\tau = \frac{\Delta x}{2c} \left( \coth(\text{Pe}) - \frac{1}{\text{Pe}} \right), \quad \text{Pe} = \frac{|c|h}{2K}, \quad \Delta x = x_i - x_{i-1} = \text{const} \quad (5.1)$$

fulfills this criterion and leads to nodally exact approximations. This formula has been generalized in a straightforward way to multi-dimensions, and is—together with similar versions—frequently used in practice for the successful stabilization of arbitrary problems with linear FEM; and this although it is derived only from the special case of the one-dimensional advection-diffusion equation. It has been shown in [16, 17] that straightforward use of this formula for higher-order FEM is not justified in general, and requires some modifications. It may thus be presumed that using these standard formulas derived in the mesh-based context of the linear FEM is also not suitable for MMs in general.

The standard way to obtain the coth-formula is to analytically solve the resulting *difference* equations in the system of equations emanating from the weak form of the model equation, discretized with linear FEM. Then, this solution is equated with the analytical solution of the *differential* equation [13, 26, 40]. An alternative way works with help of a Taylor series expansion [15]. In the following, another approach is presented, see also [20, 21]. We find this approach particularly useful to determine nodally exact solutions of the one-dimensional advection-diffusion equation with arbitrary (not only linear) finite element interpolations, and also with MMs. For a comparison of different possibilities to obtain formulas for  $\tau$  see [20].

## 5.1 Standard Formulas for $\tau$

In practice, alternative versions of the stabilization parameter are used instead of the "optimal" coth-version (5.1), which is due to the fact that they are less time-consuming to compute. They can be considered as approximations of the coth-formula and are compared in Fig. 4. Instead of

$$\tau = \frac{\Delta x}{2c} \left( \coth(\text{Pe}) - \frac{1}{\text{Pe}} \right) = \frac{\Delta x}{2c} \omega, \quad (5.2)$$

only  $\omega$  ("diffusion correction factor" [53]) is visualized as a function of the element Peclet number.

- optimal version, first in [13]

$$\omega = \left( \coth(\text{Pe}) - \frac{1}{\text{Pe}} \right) \quad (5.3)$$

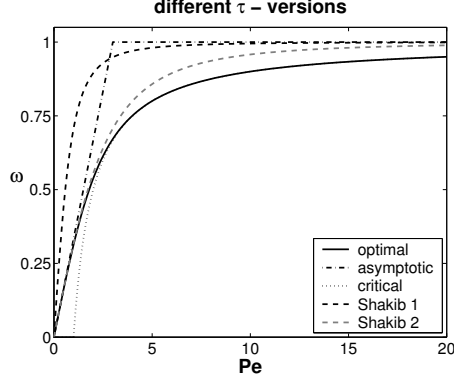


Figure 4: Alternative versions of the stabilization parameter  $\tau = \frac{\Delta x}{2c}\omega$ .

- doubly asymptotic approximation [10, 32]

$$\omega = \begin{cases} \text{Pe}/3, & -3 \leq \text{Pe} \leq 3 \\ \text{sgn}(\text{Pe}), & \text{Pe} > 3 \end{cases} \quad (5.4)$$

- critical approximation [10, 13, 32]

$$\omega = \begin{cases} -1 - 1/\text{Pe}, & \text{Pe} < -1 \\ 0, & -1 \leq \text{Pe} \leq 1 \\ 1 - 1/\text{Pe}, & \text{Pe} > 1 \end{cases} \quad (5.5)$$

- versions of Shakib [53]

$$\omega_1 = \left(1 + \frac{1}{\text{Pe}^2}\right)^{-1/2}, \quad \omega_2 = \left(1 + \frac{9}{\text{Pe}^2}\right)^{-1/2} \quad (5.6)$$

The first version of Shakib,  $\omega_1$ , is maybe the one most often used in practice:

$$\tau = \frac{\Delta x}{2c}\omega_1 = \frac{\Delta x}{2c} \left(1 + \frac{1}{\text{Pe}^2}\right)^{-1/2} = \left[ \left(\frac{2c}{\Delta x}\right)^2 + \left(\frac{4K}{\Delta x^2}\right)^2 \right]^{-1/2}. \quad (5.7)$$

The two terms in the right expression can be interpreted as the advection-dominated and diffusion-dominated limit [56]. It can be seen that the dependency on the mesh size  $\Delta x$  in the advection-dominated case is  $\tau \approx \frac{\Delta x}{2c}$ , hence  $O(\Delta x)$ , while it is in the diffusion-dominated case  $\tau \approx \frac{\Delta x^2}{4K}$ , hence  $O(\Delta x^2)$ . In multi-dimensions the parameter  $\Delta x$  is replaced by suitable length measures, in the finite element context in general by the element length  $h_e$ . For instationary problems an additional time term of  $\left(\frac{2}{\Delta t}\right)^2$  is added in (5.7). The resulting formula is used in part II of this work [22], whereas here the coth-formula is used.

## 5.2 One-Dimensional Advection-Diffusion Equation

The strong form of the one-dimensional advection-diffusion equation is

$$c \frac{\partial u(x)}{\partial x} - K \frac{\partial^2 u(x)}{\partial x^2} = 0, \quad x \in \Omega; c, K \in \mathbb{R}, \quad (5.8)$$

with suitable boundary conditions. A scalar quantity  $u(x)$  is advected with the velocity  $c$  and thereby experiences diffusion dependent on  $K$ . The exact solution of this problem is known as

$$u^{(\text{ex})} = C_1 e^{\gamma x} + C_2, \quad \gamma = \frac{c}{K}. \quad (5.9)$$

MLS nodes are introduced at the positions  $x_1, x_2, \dots, x_n$  inside the domain. Discretization of the SUPG stabilized weak form with  $\tilde{u}(x) = \mathbf{N}^T(x) \mathbf{u}$  gives

$$\int_{\Omega} (\mathbf{w} + \tau c \cdot \partial_x \mathbf{w}) (c \cdot \partial_x \tilde{u} - K \partial_x^2 \tilde{u}) d\Omega = \mathbf{0}, \quad (5.10)$$

where  $\partial_x = \partial/\partial x$ .

Let us extract one equation—say equation no.  $\ell$ —of this system of equations,

$$\left[ \int_{\Omega} (w_{\ell} + \tau_{\ell} c \cdot \partial_x w_{\ell}) (c \cdot \partial_x \mathbf{N}^T - K \partial_x^2 \mathbf{N}^T) d\Omega \right] \mathbf{u} = \mathbf{0}. \quad (5.11)$$

This equation corresponds to node  $\ell$  at  $x_{\ell}$  with the test function  $w_{\ell}$ . There is one  $\tau_{\ell}$  for each equation/node. Consequently, one may call this stabilization *nodal stabilization*, in contrast to element stabilization—where stabilization parameters  $\tau_e$  for each element matrix are used—which is standard in the FEM. See [20] for a detailed comparison of nodal and element stabilization.

The  $\tau_{\ell}$ -values of each equation are computed such that the nodally exact solution is obtained. This can be done by introducing the exact solution into the vector  $\mathbf{u}$ . We have  $u^{(\text{ex})}(x_j) = u_j^{(\text{ex})} = C_1 e^{\gamma x_j} + C_2$ , and according to the ansatz  $\tilde{u}(x_j) = \tilde{u}_j = \sum N_i(x_j) u_i$ . Nodal exactness means

$$\begin{aligned} \tilde{u}_j &= u_j^{(\text{ex})}, \\ \sum N_i(x_j) u_i &= C_1 e^{\gamma x_j} + C_2, \\ \mathbf{D} \mathbf{u} &= \mathbf{u}^{(\text{ex})}, \end{aligned} \quad (5.12)$$

where  $\mathbf{D} = D_{ij} = N_i(x_j)$  is a  $n \times n$  matrix of the  $n$  shape functions evaluated at the  $n$  nodal positions.  $\mathbf{D}$  is a sparse matrix if the shape functions are non-zero only in small parts of the domain  $\Omega$ . In the FEM, the shape functions have local supports, specified indirectly with help of the mesh, whereas the supports of MMs are defined with help of the dilatation parameter  $\rho$  [19]. For shape functions with Kronecker- $\delta$  property,  $N_i(x_j) = \delta_{ij}$  and thus  $\mathbf{D} = \mathbf{I}$ .

Rearranging (5.11) for  $\tau_{\ell}$  and replacing  $\mathbf{u}$  with  $\mathbf{D}^{-1} \mathbf{u}^{(\text{ex})}$  results in

$$\begin{aligned} \tau_{\ell} &= - \frac{[\int_{\Omega} (w_{\ell}) (c \cdot \partial_x \mathbf{N}^T - K \partial_x^2 \mathbf{N}^T) d\Omega] \mathbf{D}^{-1} \mathbf{u}^{(\text{ex})}}{[\int_{\Omega} (c \cdot \partial_x w_{\ell}) (c \cdot \partial_x \mathbf{N}^T - K \partial_x^2 \mathbf{N}^T) d\Omega] \mathbf{D}^{-1} \mathbf{u}^{(\text{ex})}} \\ &= - \frac{[\int_{\Omega} (w_{\ell}) (c \cdot \partial_x \mathbf{N}^T \mathbf{D}^{-1} - K \partial_x^2 \mathbf{N}^T \mathbf{D}^{-1}) d\Omega] \mathbf{u}^{(\text{ex})}}{[\int_{\Omega} (c \cdot \partial_x w_{\ell} \partial_x) (c \cdot \partial_x \mathbf{N}^T \mathbf{D}^{-1} - K \partial_x^2 \mathbf{N}^T \mathbf{D}^{-1}) d\Omega] \mathbf{u}^{(\text{ex})}}. \end{aligned} \quad (5.13)$$

This expression for  $\tau_\ell$  leads to nodally exact solutions for arbitrary shape and test functions and arbitrary point distributions. In what follows, this result will be interpreted.

### 5.3 Linear FEM

In the case of linear finite element shape functions, a number of simplifications for (5.13) is possible. Due to the Kronecker- $\delta$  property of the nodal finite element shape functions, we have  $\mathbf{D} = \mathbf{D}^{-1} = \mathbf{I}$ . Partial integration is applied to the diffusion term in the nominator, whereas this term cancels out in the denominator (assuming that the second derivatives of the linear finite element shape functions are 0 everywhere in  $\Omega$ ). It remains for  $\tau_\ell$  (for constant  $c$  and  $K$ ):

$$\begin{aligned}\tau_\ell &= -\frac{[c \int_\Omega w_\ell \partial_x \mathbf{N}^T d\Omega + K \int_\Omega \partial_x w_\ell \partial_x \mathbf{N}^T d\Omega] \mathbf{u}^{(\text{ex})}}{[c^2 \int_\Omega \partial_x w_\ell \partial_x \mathbf{N}^T d\Omega] \mathbf{u}^{(\text{ex})}}, \\ &= -\frac{[c \int_\Omega w_\ell \partial_x \mathbf{N}^T d\Omega] \mathbf{u}^{(\text{ex})}}{[c^2 \int_\Omega \partial_x w_\ell \partial_x \mathbf{N}^T d\Omega] \mathbf{u}^{(\text{ex})}} - \frac{K}{c^2}.\end{aligned}\tag{5.14}$$

The integral expressions in (5.14) can be evaluated explicetly for the case of linear shape and test functions and a regular node distribution as

$$\int_\Omega w_\ell \partial_x \mathbf{N}^T d\Omega = \frac{1}{2} \begin{bmatrix} -1, & 0, & 1 \end{bmatrix},\tag{5.15}$$

$$\int_\Omega \partial_x w_\ell \partial_x \mathbf{N}^T d\Omega = \frac{1}{\Delta x} \begin{bmatrix} -1, & 2, & -1 \end{bmatrix}.\tag{5.16}$$

The scalar product of these expressions with  $\mathbf{u}^{(\text{ex})} = C_1 e^{\gamma \cdot \mathbf{x}} + C_2$  gives

$$\begin{aligned}\tau_\ell &= \frac{\Delta x}{2c} \frac{E_{\ell+1} - E_{\ell-1}}{E_{\ell-1} + 2E_\ell + E_{\ell+1}} - \frac{K}{c^2}, \\ &= \frac{\Delta x}{2c} \frac{\sinh(\gamma \Delta x)}{\cosh(\gamma \Delta x) - 1} - \frac{K}{c^2}, \\ &= \frac{\Delta x}{2c} \left( \coth(\text{Pe}) - \frac{1}{\text{Pe}} \right),\end{aligned}\tag{5.17}$$

with  $E_j = C_1 e^{\gamma \cdot x_j} + C_2$  and  $\text{Pe} = \gamma \cdot \Delta x / 2 = c \cdot \Delta x / (2K)$ . With this definition of the stabilization parameter one obtains the nodally exact solution for the one-dimensional advection-diffusion equation, approximated with linear FEM and a regular node distribution. Using standard element stabilization instead of nodal stabilization with  $\tau_e = \tau_\ell$  leads to the same result. This formula for  $\tau$  has often be called 'optimal' in the literature, e.g. in [10, 13, 26, 40]. It has a *local* character as it is independent of the boundary conditions and only relies on the relative positions of the neighbouring nodes  $x_{\ell-1}$  and  $x_{\ell+1}$ . Although it is derived for the very special case of the one-dimensional advection-diffusion equation approximated with linear finite elements and a regular node distribution, it has been generalized straightforward to instationary multi-dimensional advection-dominated problems approximated with linear FEM in arbitrary nodal arrangements.

**Remark 2** This procedure for determining formulas for  $\tau$  may be applied analogously to higher order elements, see [20]. Thereby nodally exact solution may be also found for higher order approximations. In these cases individual formulas for  $\tau$  for each line of the element matrix are

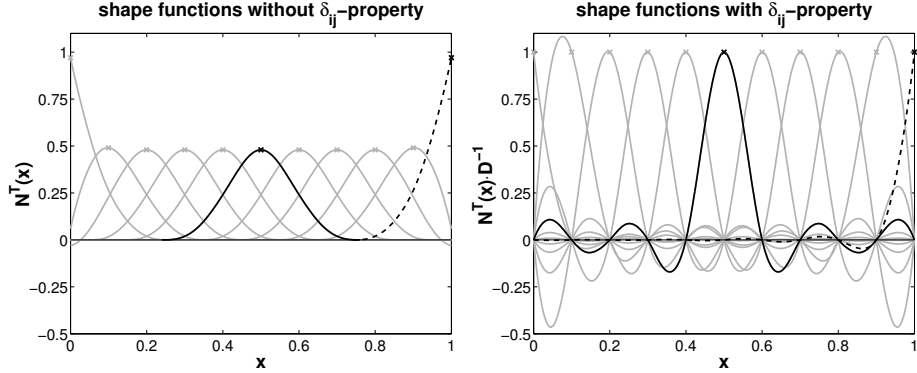


Figure 5: Local shape functions  $\mathbf{N}^T$  without Kronecker- $\delta$  property and transformed global shape functions  $\mathbf{N}^T \mathbf{D}^{-1}$  with Kronecker- $\delta$  property.

obtained. Using standard formulas for  $\tau$  derived for linear shape functions may not be well-suited here, see also [16, 17].

## 5.4 Meshfree Methods

For meshfree methods, (5.13) can not be simplified in general. This result is interpreted as follows. Let us rewrite the expression for  $\tau_\ell$  as

$$\tau_\ell = - \frac{[\int_\Omega f_1(w_\ell) g(\mathbf{N}^T \mathbf{D}^{-1}) d\Omega] \mathbf{u}^{(\text{ex})}}{[\int_\Omega f_2(w_\ell) g(\mathbf{N}^T \mathbf{D}^{-1}) d\Omega] \mathbf{u}^{(\text{ex})}}, \quad (5.18)$$

where  $f_1$ ,  $f_2$  and  $g$  are linear functions of the test and shape functions respectively. The expressions in the nominator and denominator are scalar products

$$\int_\Omega \underbrace{f_i(w_\ell)}_{1 \times 1} \underbrace{g(\mathbf{N}^T \mathbf{D}^{-1})}_{1 \times n} d\Omega \underbrace{\mathbf{u}^{(\text{ex})}}_{n \times 1}. \quad (5.19)$$

The meshfree test and shape functions  $\mathbf{w}$  and  $\mathbf{N}$  have local supports. However, the term  $\mathbf{N}^T \mathbf{D}^{-1}$  can be interpreted as the 'globalized' meshfree shape functions having Kronecker- $\delta$  property. This may be gleaned from Fig. 5, where local shape functions  $\mathbf{N}^T$  without and transformed global shape functions  $\mathbf{N}^T \mathbf{D}^{-1}$  with Kronecker- $\delta$  property are shown.

**Remark 3** It is well known [43] that locally defined meshfree MLS shape functions with Kronecker- $\delta$  property require singular weighting functions in the MLS procedure. This however has a number of severe numerical disadvantages and is only rarely used in practice.

Consequently, the vectors  $\int_\Omega f_i(w_\ell) g(\mathbf{N}^T \mathbf{D}^{-1}) d\Omega$  are full vectors, which is in contrast to shape functions having Kronecker- $\delta$  property. In the latter case,  $g(\mathbf{N}^T \mathbf{D}^{-1}) = g(\mathbf{N}^T)$ , and the vector is sparse. Evaluating the scalar product with  $\mathbf{u}^{(\text{ex})}$  shows the important difference: Shape functions without Kronecker- $\delta$  property have non-zero entries in the scalar-product for *all* components of the vector  $\mathbf{u}^{(\text{ex})}$ , whereas, in contrast, shape functions with Kronecker- $\delta$  property only have non-zero entries for the *neighbouring* nodes. This may be seen symbolically from Fig. 6,

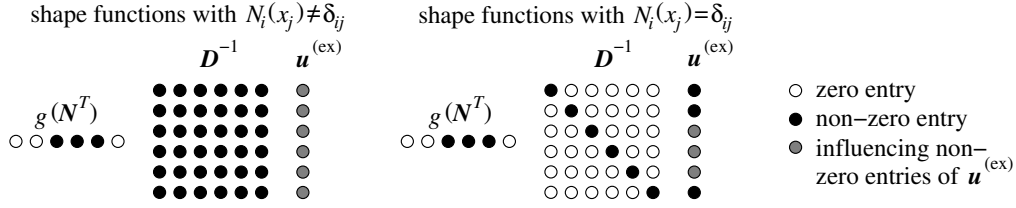


Figure 6: Evaluating the scalar products for  $\tau_\ell$  for shape function without and with Kronecker- $\delta$  property, in the former case all entries of  $\mathbf{u}^{(\text{ex})}$  have influence in the result.

where it is clear that the nodally exact  $\tau_\ell$  for shape functions without Kronecker- $\delta$  property can only be obtained with a global criterion, because all entries of  $\mathbf{u}^{(\text{ex})}$  have an influence on the result.

Keeping in mind that  $\mathbf{u}^{(\text{ex})}$  is an exponential function, the scalar product will depend more and more on the last entry of this vector as the convection-diffusion ratio  $\gamma = c/K$  grows, because then

$$u^{(\text{ex})}(x_n) = u_n^{(\text{ex})} \gg u_i^{(\text{ex})} = u^{(\text{ex})}(x_i) \quad \forall i \neq n. \quad (5.20)$$

The last component of  $\mathbf{u}^{(\text{ex})}$  is  $u_n^{(\text{ex})}$ , and belongs to node  $n$  with the largest  $x$ -value, i.e. the global downstream node. The conclusion is that the stabilization parameter  $\tau_\ell$ , leading to nodally exact solutions has a *global* character, as it depends on all node positions and for convection-dominated cases most importantly on the global downstream node. This is in contrast to shape functions with Kronecker- $\delta$  property, whose stabilization relies on the neighbouring nodes only. Therefore, it can in general not be expected that using the simple coth-formula—or other alternative similar versions derived as a local stabilization criterion for linear FEM—is successful also for MMs.

## 5.5 Small Dilatation Parameters

Meshfree shape functions are constructed with help of the node distribution and the definition of supports, see section 2. The support sizes are defined by the dilatation parameter  $\rho_i$ . It is a well known fact that MLS shape functions in one dimension with first order consistency become more and more equal to the standard nodal linear shape functions of the FEM as the dilatation parameter  $\rho$  approaches  $\Delta x$ . This is also shown in Fig. 7. Hence it may be concluded that when  $\rho \rightarrow \Delta x$ , the coth-formula becomes more and more suited also for MMs. Hence

$$\rho \rightarrow 1 \cdot \Delta x \quad : \quad \mathbf{N}^{(\text{MM})} \rightarrow \mathbf{N}^{(\text{lin FEM})} \quad (5.21)$$

$$\Rightarrow \tau_\ell^{(\text{MM})} \rightarrow \tau_\ell^{(\text{lin. FEM})} = \frac{\Delta x}{2c} \left( \coth(\text{Pe}) - \frac{1}{\text{Pe}} \right). \quad (5.22)$$

A stability criterion of the MLS requires  $\rho > \Delta x$  for linear consistency [46]. Thus, one can never reach the limit  $\rho = \Delta x$ , where the coth-formula gives the nodally exact solution. We propose however that for reasonable advection-diffusion ratios and 'small' dilatation parameters a successful stabilization with standard formulas—derived for mesh-based methods—can be obtained. We suggest dilatation parameters of  $1.3\Delta x \leq \rho \leq 1.7\Delta x$ . For smaller  $\rho$ , the condition number of the MLS system of equations which has to be solved at every integration point may be too large to

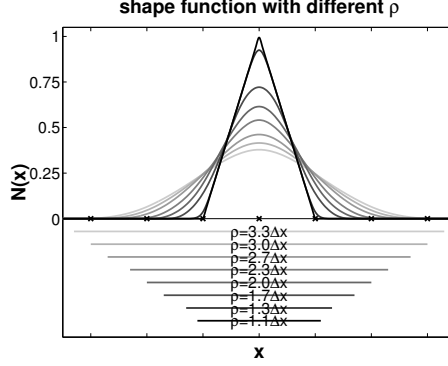


Figure 7: Meshfree shape function in a regular node distribution with varying dilatation parameter  $\rho$ .

allow a sufficiently accurate solution, and for larger  $\rho$  the stabilization may not be reliable. The numerical results in section 6 confirm this assumption.

## 5.6 Stabilization Parameter in Multi-Dimensions

In the FEM, i.e. in the mesh-based context, the generalization of the  $\tau$ -formulas derived from the one-dimensional advection-diffusion equation to multi-dimensions is straightforward [10]. The one-dimensional parameters  $\Delta x$  and  $c$  are replaced with the element length  $h_e$  and the norm of the advection  $|\mathbf{c}|$ . Assuming small dilatation parameters, the same generalization is proposed for meshfree methods. Hence  $\tau_\ell$  in multi-dimensions may be computed with

$$\tau_\ell = \frac{h_\rho}{2|\mathbf{c}|} \left( \coth(\text{Pe}_\rho) - \frac{1}{\text{Pe}_\rho} \right) \quad \text{with } \text{Pe}_\rho = \frac{|\mathbf{c}| h_\rho}{2K} \quad (5.23)$$

or any other of the alternative versions for  $\tau$ , see subsection 5.1. Here  $h_\rho$  is the 'support length', analogously to the 'element length'  $h_e$  in the mesh-based context.

- min-version:

$$h_\rho = \min(\rho_x, \rho_y) \quad (5.24)$$

- max-version:

$$h_\rho = \max(\rho_x, \rho_y) \quad (5.25)$$

- inner-ellipsoid-version:

$$h_\rho = \sqrt{\frac{\left(1 + \frac{c_y^2}{c_x^2}\right) \cdot \rho_y^2}{\left(\frac{c_y}{c_x}\right)^2 + \left(\frac{\rho_y}{\rho_x}\right)^2}} \quad (5.26)$$

- real-length-version:

$$h_\rho = \min\left(\frac{\rho_x}{|c_x|}, \frac{\rho_y}{|c_y|}\right) \cdot \sqrt{c_x^2 + c_y^2} \quad (5.27)$$

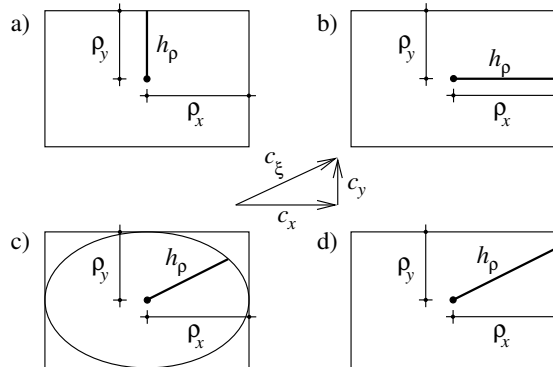


Figure 8: Different versions to compute the support length in streamline direction; a) min-version, b) max-version, c) inner-ellipsoid-version, d) real-length-version.

Fig. 8 shows several possibilities to interpret  $h_\rho$  in case of rectangular supports. The support lengths for circular and ellipsoid supports can be directly read of from these formulas.

In case of the incompressible Navier-Stokes equations in two dimensions, the advection coefficients  $\mathbf{c} = (c_x, c_y)$  are replaced by the convective velocities  $\mathbf{u} = (u, v)$ . In case of the ALE formulated Navier-Stokes equations [38], used in part II of this work [22], the convective velocity is  $\bar{\mathbf{u}} = \mathbf{u} - \boldsymbol{\chi}$ , where  $\boldsymbol{\chi}$  is the mesh velocity. In the numerical experiments it is found that particularly the min-version (5.24) works very successfully also for large aspect ratios ( $\rho_x/\rho_y \gg 1$ , or  $\rho_y/\rho_x \gg 1$ ). See Mittal [47] for an interesting parallel for high aspect *elements*: He also finds that the minimal edge length works better than other versions for  $h_e$ .

The inner-ellipsoid-version (5.26) and the real-length-version (5.27) are dependent of the streamline direction of the flow inside the support. In case of the incompressible Navier-Stokes equations, this introduces some disadvantages: A representative streamline direction has to be found for the whole support, the streamline direction changes with each iteration and/or time step, and the non-linearity introduced by  $\tau = f(u, v, h_\rho)$  is more complex as compared with the min- (5.24) and max-version (5.25).

## 6 Numerical Results

Numerical results are shown for two different problems. The first is the one-dimensional advection-diffusion equation (5.8), the model equation of subsection 5.2. It is shown that nodally exact solutions with meshfree shape functions are obtained, but a global stabilization criterion is needed. Then, it is shown that standard formulas for  $\tau$  are successful only for small dilatation parameters, which confirms our assumption from subsection 5.5 due to (5.22).

The second problem are the incompressible Navier-Stokes equations in two dimensions (3.9). SUPG/PSPG and GLS stabilization according to (4.1) and (4.2) is applied and compared. Small dilatation parameters are a crucial ingredient to obtain successfully stabilized results. Using supports with too large dilatation parameters results in degradation of convergence and solutions that are still either too oscillatory or too diffusive. Our intention is to show that stabilization with small dilatation parameters

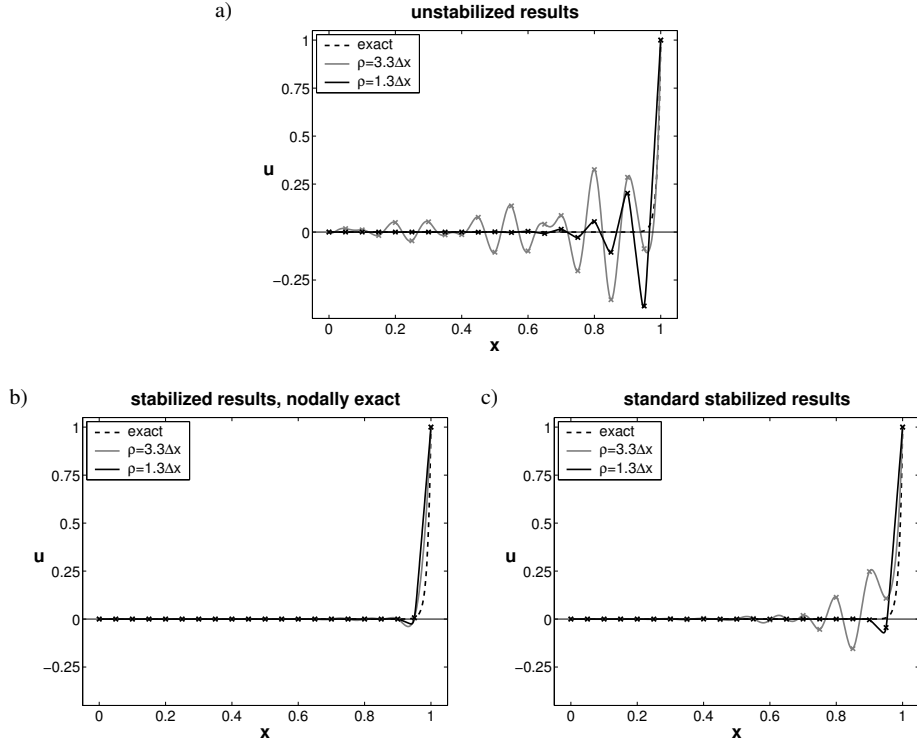


Figure 9: Results for the 1D advection-diffusion equation; a) without any stabilization, b) with the global stabilization criterion (5.13), c) with the local coth-formula (5.17).

- smoothes out oscillations successfully
- does not degrade accuracy in cases where stabilization is not necessary
- works also for anisotropic supports.

## 6.1 One-dimensional Advection-Diffusion Equation

The one-dimensional advection diffusion equation (5.8) is solved with 21 MLS nodes. The advection-diffusion ratio is  $\gamma = c/K = 100$ . Fig. 9a) shows the unstabilized results for two different dilatation parameters  $\rho = 1.3\Delta x$  ("small") and  $\rho = 3.3\Delta x$  ("large"). It can be seen that higher dilatation parameters lead to more oscillations, simply due to their higher Peclet number,  $Pe_\rho = \frac{c\rho}{2K}$ . Clearly, for both cases, stabilization is required.

Fig. 9b) shows the nodally exact result, which can be obtained with the global stabilization criterion for  $\tau_\ell$ , see (5.13). In Fig. 9c) it can be seen that standard formulas for  $\tau_\ell$  like the coth-formula

$$\tau_\ell = \frac{h_\rho}{2c} \left( \coth(Pe_\rho) - \frac{1}{Pe_\rho} \right) \quad (6.1)$$

only lead to successful stabilization when the dilatation parameter is small. Comparison of Fig. 9b) and c) shows that for small dilatation parameters, the result of the complicated global criterion (5.13) and the coth-criterion (5.17) gives almost the same result. This, however, is not the case for the large dilatation parameter of  $\rho = 3.3\Delta x$ , where pronounced oscillations remain in the solution.

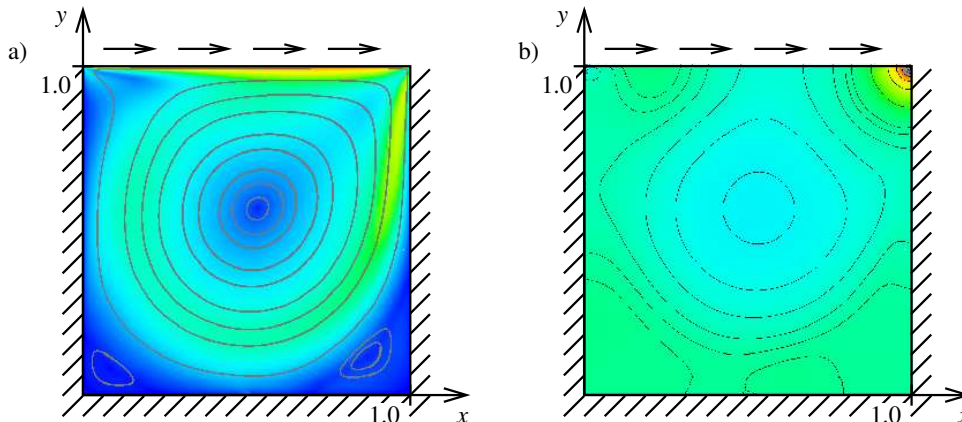


Figure 10: Problem statement of the driven cavity test case. As an example the a) velocity magnitude and b) pressure field is shown at  $Re = 1000$ .

These oscillations are clearly not a problem of the high gradient itself that could not be captured by shape functions with such a large dilatation parameter (then the result of Fig. 9b should have been oscillatory, too, and this is not the case), but results from the use of unsuitable stabilization parameters.

The conclusion is that the assumption of subsection 5.5 is confirmed: Standard formulas of meshbased methods for the stabilization parameter  $\tau$  can only be reliably used for MMs with small dilatation parameters.

## 6.2 Incompressible Navier-Stokes Equations

### 6.2.1 Driven Cavity Flow

The driven cavity problem is a standard test case with reference solutions given in [23] for a variety of Reynolds numbers. A flow field develops in a unit square under the influence of a horizontal shear flow applied along the upper wall, and on the other three walls no-slip boundary conditions are applied. Herein, this problem is solved with  $Re = 1000$ . For a problem statement see Fig. 10, showing also streamlines and pressure distribution for  $Re = 1000$ . In the sequel, only *velocity profiles* are studied at certain cuts through the two-dimensional domain.

The first results are produced with  $21 \times 21$  regularly distributed MLS nodes. Fig. 11 shows velocity profiles for  $u$  and  $v$  at  $y = 0.95$ , i.e. near the tangential flow boundary, where most of the oscillations occur. Two different dilatation parameters are shown,  $\rho = 1.3\Delta x$  and  $\rho = 2.3\Delta x$ . Dilatation parameters  $\rho > 2.7\Delta x$  converged either not at all or only very badly, underlining the need for small dilatation parameters, when standard formulas for  $\tau_\ell$  are used.

One can clearly see that the oscillations apparent in the unstabilized result are smoothed out successfully, especially for the case where  $\rho = 1.3\Delta x$ . For  $\rho = 2.3\Delta x$  one may see from the velocity profile for  $v$  that very slight oscillations remain in this case. Again, the assumption that shape functions with small dilatation parameters can be stabilized very successfully is confirmed.

Fig. 12 shows the center velocity profiles for the case where  $\rho = 1.3\Delta x$ . Although along these cuts no oscillations are apparent in the unstabilized case, the stabilized profiles give better

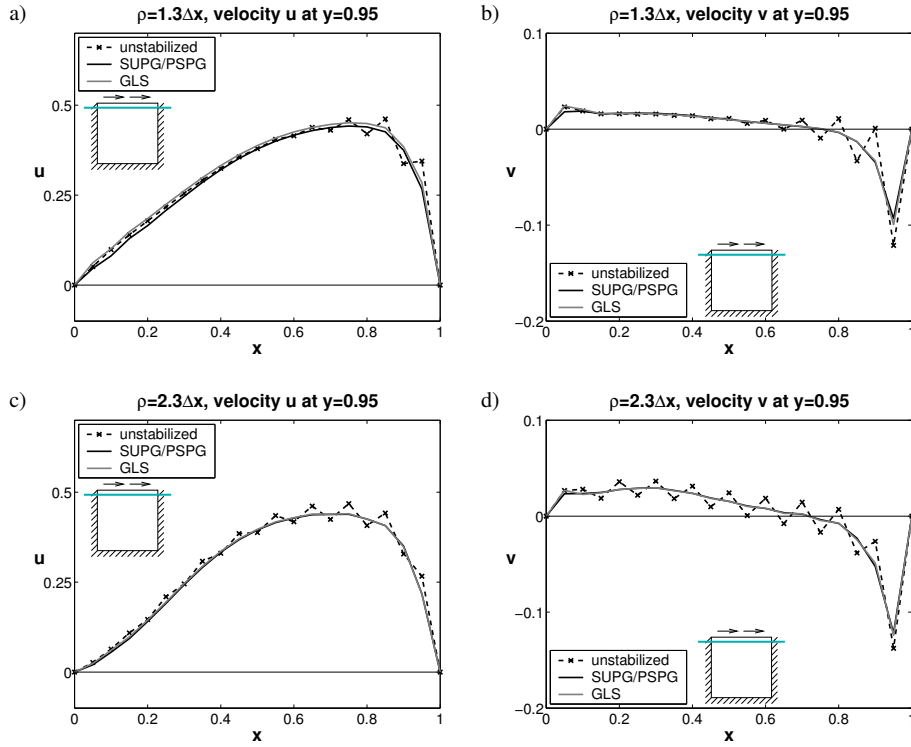


Figure 11: Velocity profiles for  $u$  and  $v$  near the tangential flow boundary at  $y = 0.95$  for different dilatation parameters of  $\rho = 1.3\Delta x$  and  $\rho = 2.3\Delta x$ .

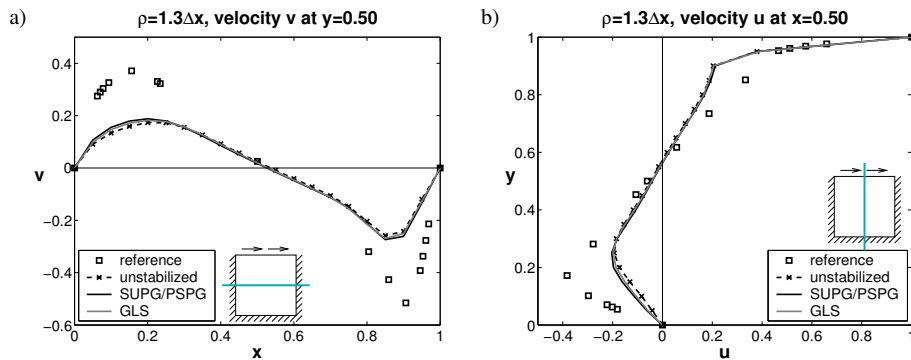


Figure 12: Velocity profiles for  $u$  and  $v$  along  $y = 0.5$  and  $x = 0.5$  respectively (for  $\rho = 1.3\Delta x$  and  $21 \times 21$  nodes).

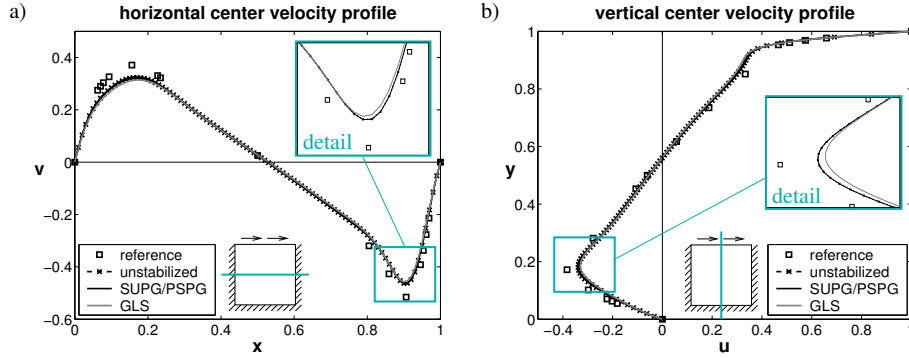


Figure 13: Velocity profiles for  $u$  and  $v$  along  $y = 0.5$  and  $x = 0.5$  respectively (for  $\rho = 1.3\Delta x$  and  $101 \times 101$  nodes). The details show that unstabilized and SUPG/PSPG-results are indistinguishable, whereas the GLS result is slightly more diffusive.

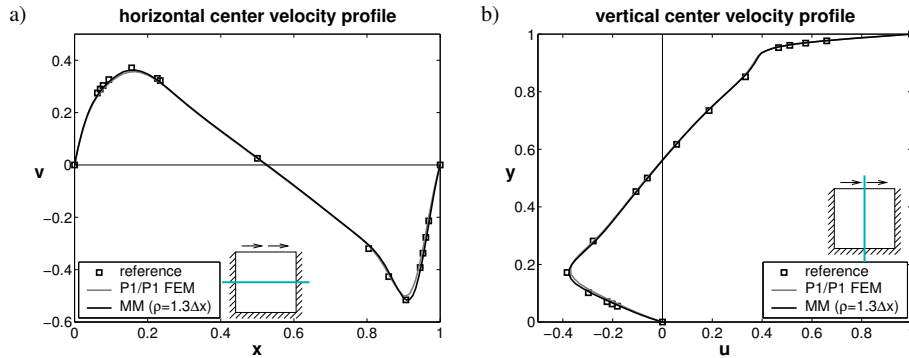


Figure 14: Velocity profiles for  $u$  and  $v$  along  $y = 0.5$  and  $x = 0.5$  respectively (for  $\rho = 1.3\Delta x$  and  $96 \times 96$  irregular nodes).

results. The reason for this is that the oscillations in the unstabilized case near the tangential flow boundary degrade the overall solution. Obviously, stabilization for shape functions with small dilatation parameters smoothes out oscillations successfully and leads to superior overall solutions than unstabilized calculations. It should be mentioned that the rather big difference to the reference solution given in [23] is due to the coarse node distribution and improves clearly for more refined distributions as shown later.

The next results are computed with  $101 \times 101$  MLS nodes and  $\rho = 1.3\Delta x$ . With this large number of nodes, stabilization is not needed at all, i.e. the unstabilized solution is already free of oscillations. The results show that stabilization does not degrade the accuracy when it is not needed. Fig. 13 shows the center velocity profiles. It is interesting that unstabilized and SUPG/PSPG stabilized results are indistinguishable, whereas GLS stabilized results are slightly more diffusive. This was confirmed in a number of additional computations.

Fig. 14 shows a comparison of the reference solution with the meshfree solution (with  $\rho = 1.3\Delta x$ ) and the solution from the P1/P1 triangular element with the same number of unknowns. For both numerical methods, SUPG/PSPG stabilization and a node distribution as shown in Fig. 15 has been used. The supports of the nodes are anisotropic with respect to the distance to

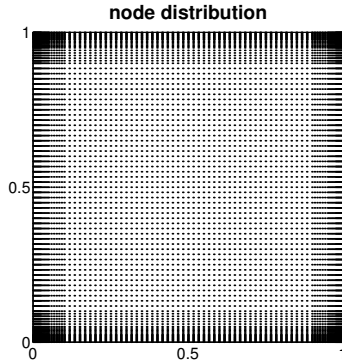


Figure 15: Node distribution with refined boundary areas for the driven cavity test case ( $96 \times 96$  nodes).

the neighboring nodes,

$$\rho_{x,i} = c \cdot \min(|x_j - x_i|), \forall i \neq j, \quad (6.2)$$

$$\rho_{y,i} = c \cdot \min(|y_j - y_i|), \forall i \neq j, \quad (6.3)$$

with  $c = 1.6$ . The min-version (5.24) for the support length  $h_\rho$  performs best when compared to the other  $h_\rho$ -versions. A clear convergence towards the reference solution can be found, and it may be seen that the meshfree solution is more accurate than the P1/P1 element. Comparing the results for the regular  $101 \times 101$  mesh with the resolved  $96 \times 96$  mesh, one can clearly see the improvement in the solution for the anisotropic supports. Hence, as well as using high-aspect ratio elements in meshbased methods in order to resolve boundary layers successfully, high-aspect anisotropic supports should be used in the meshfree context analogously.

### 6.2.2 Flow Past a Cylinder

The "steady-state" solution for flow past a cylinder at  $\text{Re} = 100$  is computed, as presented in [54]. Instationary computations at this Reynolds-number lead to periodic flow patterns known as the Kármán vortex street, this is considered in the instationary computations in part II of this work [22]. This, however, is not considered here, because in this part of the work we only aim to show the smoothing properties of the stabilization.

Inflow and outflow boundary conditions are applied on the left and right side of the rectangular domain respectively. Slip boundary conditions are applied at the upper and lower boundary, no-slip boundary conditions are applied at the cylinder surface. The cylinder is placed as shown in Fig. 16, where also the irregular node distribution for this test case is shown. Fig. 17 shows a typical result for the velocity and pressure distribution around the cylinder. Further details of this test case are not described, because our interest is rather in the stabilization characteristics than in obtaining benchmark solutions.

The supports of the meshfree shape functions are anisotropic as defined above for the irregular driven cavity test case. Fig. 18 depicts oscillatory unstabilized velocity profiles for  $u$  and  $v$  at  $y = 5.6$ . Both, SUPG/PSPG and GLS stabilization smooth out the oscillations successfully.

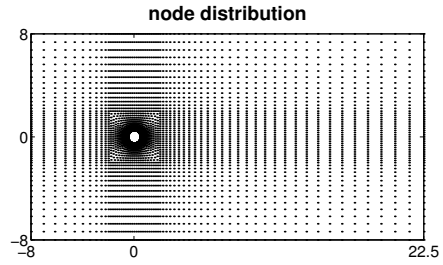


Figure 16: Irregular node distribution for the flow past a cylinder test case (6268 nodes).

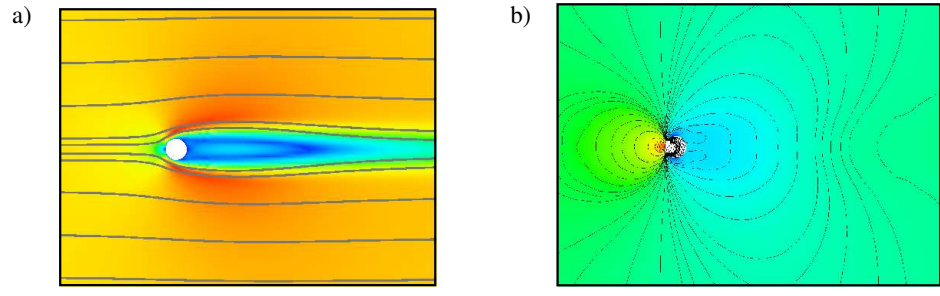


Figure 17: Detail of the stationary solution of the a) velocity and b) pressure field around the cylinder at  $Re = 100$ .

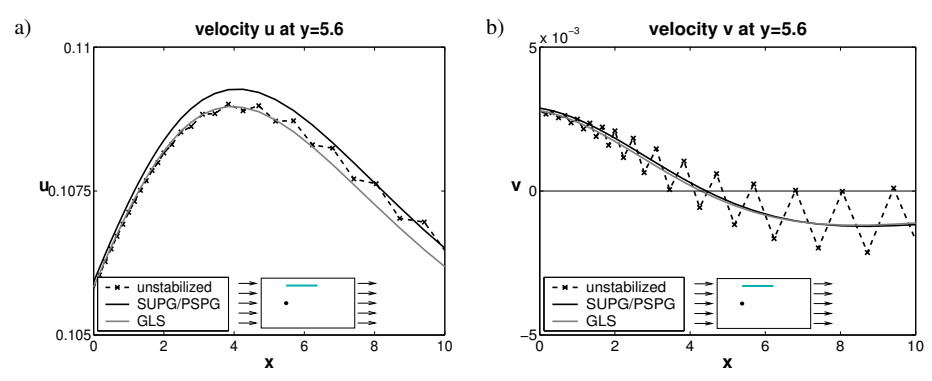


Figure 18: Velocity profiles for  $u$  and  $v$  at  $y = 5.6$ .

The conclusion is that the stabilization with small dilatation parameters works successfully also for anisotropic supports.

## 7 Conclusion

In this paper, meshfree Galerkin methods are established for the solution of flow problems in Eulerian formulation, and all conclusions may be directly extended to arbitrary Lagrangian-Eulerian (ALE) formulations. To apply these methods successfully the problem of stabilization has to be solved. The need for stabilization of the incompressible Navier-Stokes equations is described, and the SUPG/PSPG and GLS stabilization methods are considered.

It is found that the structure of these stabilization methods, i.e. the way they add perturbation terms to the weak form, can be applied to meshbased as well as to meshfree methods. However, the aspect of the stabilization parameter  $\tau$ , being a crucial ingredient in stabilized methods, has to be reconsidered. A new way is shown how to derive formulas for  $\tau$  for arbitrary shape functions. The well-known coth-formula for  $\tau$ —being the basis of many alternative versions of  $\tau$ -formulas—is obtained in the special case of linear finite element shape functions. This coth-formula is a local stabilization criterion, however applying the same methodology to meshfree methods results in a global criterion. That is, there is a dependence of  $\tau$  on all nodes, most importantly the global downstream node. In contrast, local stabilization criteria only rely on the relative positions of neighboring nodes. Therefore, it can not be expected in general that standard formulas for  $\tau$ , derived in the meshbased context, work also successfully with meshfree methods, especially not for non-linear instationary problems. However, it is found that the use of these formulas is justified for small dilatation parameters. The numerical results agree very well with our theoretical approach.

Being able to use Eulerian meshfree methods in stabilized Galerkin settings, totally analogously to meshbased standard FEM, opens the door to couple both methods for the solution of the incompressible Navier-Stokes equations. This will be considered in part II of this work [22]. Then, accurate and robust simulations may be performed with only little extra effort compared to purely meshbased computations. This stabilized and coupled fluid solver enables the solution of complex flow phenomena including moving and rotating objects, where meshes may only be hardly maintainable, and will be treated in part II.

## References

- [1] Atluri, S.N.; Shen, S.: *The Meshless Local Petrov-Galerkin (MLPG) Method*. Tech Science Press, Stuttgart, 2002.
- [2] Babuška, I.: Error-bounds for finite element method. *Numer. Math.*, **16**, 322 – 333, 1971.
- [3] Babuška, I.; Banerjee, U.; Osborn, J.E.: Meshless and generalized finite element methods: A survey of some major results. In *Meshfree Methods for Partial Differential Equations*. (Griebel, M.; Schweitzer, M.A., Eds.), Vol. 26, Springer Verlag, Berlin, 2002.

- [4] Babuška, I.; Banerjee, U.; Osborn, J.E.: Survey of meshless and generalized finite element methods: A unified approach. Technical Report 02-40, TICAM, The University of Texas at Austin, 2002.
- [5] Beissel, S.; Belytschko, T.: Nodal integration of the element-free Galerkin method. *Comp. Methods Appl. Mech. Engrg.*, **139**, 49 – 74, 1996.
- [6] Belytschko, T.; Guo, Y.; Liu, W.K.; Xiao, S.P.: A unified stability analysis of meshless particle methods. *Internat. J. Numer. Methods Engrg.*, **48**, 1359 – 1400, 2000.
- [7] Belytschko, T.; Krongauz, Y.; Organ, D.; Fleming, M.; Krysl, P.: Meshless Methods: An Overview and Recent Developments. *Comp. Methods Appl. Mech. Engrg.*, **139**, 3 – 47, 1996.
- [8] Belytschko, T.; Lu, Y.Y.; Gu, L.: Element-free Galerkin Methods. *Internat. J. Numer. Methods Engrg.*, **37**, 229 – 256, 1994.
- [9] Brezzi, F.: On the existence, uniqueness and approximation of saddle-point problems arising from Lagrange multipliers. *RAIRO Anal. Numér.*, **R-2**, 129 – 151, 1974.
- [10] Brooks, A.N.; Hughes, T.J.R.: Streamline upwind/Petrov-Galerkin formulations for convection dominated flows with particular emphasis on the incompressible Navier-Stokes equations. *Comp. Methods Appl. Mech. Engrg.*, **32**, 199 – 259, 1982.
- [11] Chen, J.S.; Wu, C.T.; You, Y.: A Stabilized Conforming Nodal Integration for Galerkin Mesh-free Methods. *Internat. J. Numer. Methods Engrg.*, **50**, 435 – 466, 2001.
- [12] Chen, J.S.; Yoon, S.; H.P. Wang, W.K. Liu: An improved reproducing kernel particle method for nearly incompressible finite elasticity. *Comp. Methods Appl. Mech. Engrg.*, **181**, 117 – 145, 2000.
- [13] Christie, I.; Griffiths, D.F.; Mitchell, A.R.; Zienkiewicz, O.C.: Finite element methods for second order differential equations with significant first derivatives. *Internat. J. Numer. Methods Engrg.*, **10**, 1389 – 1396, 1976.
- [14] Dolbow, J.; Belytschko, T.: Volumetric locking in the element free Galerkin method. *Internat. J. Numer. Methods Engrg.*, **46**, 925 – 942, 1999.
- [15] Donea, J.; Huerta, A.: *Finite Element Methods for Flow Problems*. John Wiley & Sons, Chichester, 2003.
- [16] Franca, L.P.; Frey, S.L.: Stabilized finite element methods: II. The incompressible Navier-Stokes equations. *Comp. Methods Appl. Mech. Engrg.*, **99**, 209 – 233, 1992.
- [17] Franca, L.P.; Frey, S.L.; Hughes, T.J.R.: Stabilized finite element methods: I. Application to the advective-diffusive model. *Comp. Methods Appl. Mech. Engrg.*, **95**, 253 – 276, 1992.
- [18] Franca, L.P.; Hughes, T.J.R.: Two classes of mixed finite element methods. *Comp. Methods Appl. Mech. Engrg.*, **69**, 89 – 129, 1988.

- [19] Fries, T.P.; Matthies, H.G.: Classification and Overview of Meshfree Methods. Informatikbericht-Nr. 2003-03, Technical University Braunschweig, (<http://opus.tu-bs.de/opus/volltexte/2003/418/>), Brunswick, 2003.
- [20] Fries, T.P.; Matthies, H.G.: A Review of Petrov-Galerkin Stabilization Approaches and an Extension to Meshfree Methods. Informatikbericht-Nr. 2004-01, Technical University of Braunschweig, (<http://opus.tu-bs.de/opus/volltexte/2004/549/>), Brunswick, 2004.
- [21] Fries, T.P.; Matthies, H.G.: Meshfree Petrov-Galerkin Methods for the Incompressible Navier-Stokes Equations. In *Meshfree Methods for Partial Differential Equations*. (Griebel, M.; Schweitzer, M.A., Eds.), Vol. 43, Springer Verlag, Berlin, 2005.
- [22] Fries, T.P.; Matthies, H.G.: A Stabilized and Coupled Meshfree/Meshbased Method for the Incompressible Navier-Stokes Equations — Part II: Coupling. Informatikbericht-Nr. 2005-03, Technical University of Braunschweig, (<http://opus.tu-bs.de/opus/volltexte/2005/678/>), Brunswick, 2005.
- [23] Ghia, U.; Ghia, K.N.; Shin, C.T.: High-Re solutions for incompressible flow using the Navier-Stokes equations and a multi-grid method. *J. Comput. Phys.*, **48**, 387 – 411, 1982.
- [24] Gresho, P.M.; Sani, R.L.: *Incompressible Flow and the Finite Element Method*, Vol. 1+2. John Wiley & Sons, Chichester, 2000.
- [25] Günther, F.C.: *A Meshfree Formulation for the Numerical Solution of the Viscous Compressible Navier-Stokes Equations*. Dissertation, Northwestern University, Evanston, IL, 1998.
- [26] Heinrich, J.C.; Huyakorn, P.S.; Zienkiewicz, O.C.; Mitchell, A.R.: An 'upwind' finite element scheme for two-dimensional convective transport equation. *Internat. J. Numer. Methods Engrg.*, **11**, 131 – 143, 1977.
- [27] Hirsch, C.: *Numerical Computation of Internal and External Flows: Computational Methods for Inviscid and Viscous Flows*, Vol. 2. John Wiley & Sons, Chichester, 1988.
- [28] Hirsch, C.: *Numerical Computation of Internal and External Flows: Fundamentals of Numerical Discretization*, Vol. 1. John Wiley & Sons, Chichester, 1988.
- [29] Huerta, A.; Fernández-Méndez, S.: Locking in the incompressible limit for the element free Galerkin method. *Internat. J. Numer. Methods Engrg.*, **50**, 1 – 23, 2001.
- [30] Huerta, A.; Fernández-Méndez, S.M.: Time accurate consistently stabilized mesh-free methods for convection-dominated problems. *Internat. J. Numer. Methods Engrg.*, **50**, 1 – 18, 2001.
- [31] Huerta, A.; Vidal, Y.; Villon, P.: Pseudo-divergence-free element free Galerkin method for incompressible fluid flow. *Comp. Methods Appl. Mech. Engrg.*, **193**, 1119 – 1136, 2004.
- [32] Hughes, T.J.R.: A simple scheme for developing 'upwind' finite elements. *Internat. J. Numer. Methods Engrg.*, **12**, 1359 – 1365, 1978.

- [33] Hughes, T.J.R.: Multiscale phenomena: Green's functions, the Dirichlet-to-Neumann formulation, subgrid scale models, bubbles and the origins of stabilized methods. *Comp. Methods Appl. Mech. Engrg.*, **127**, 387 – 401, 1995.
- [34] Hughes, T.J.R.; Brooks, A.N.: A multidimensional upwind scheme with no crosswind diffusion. In *ASME Monograph AMD-34*. (Hughes, T.J.R., Ed.), Vol. 34, ASME, New York, NY, 1979.
- [35] Hughes, T.J.R.; Franca, L.P.: A new finite element formulation for computational fluid dynamics: VII. The Stokes problem with various well-posed boundary conditions: symmetric formulations that converge for all velocity/pressure spaces. *Comp. Methods Appl. Mech. Engrg.*, **65**, 85 – 96, 1987.
- [36] Hughes, T.J.R.; Franca, L.P.; Balestra, M.: A new finite element formulation for computational fluid dynamics: V. Circumventing the Babuška-Brezzi condition: a stable Petrov-Galerkin formulation of the Stokes problem accommodating equal-order interpolations. *Comp. Methods Appl. Mech. Engrg.*, **59**, 85 – 99, 1986.
- [37] Hughes, T.J.R.; Franca, L.P.; Hulbert, G.M.: A new finite element formulation for computational fluid dynamics: VIII. The Galerkin/Least-squares method for advective-diffusive equations. *Comp. Methods Appl. Mech. Engrg.*, **73**, 173 – 189, 1989.
- [38] Hughes, T.J.R.; Liu, W.K.; Zimmermann, T.K.: Lagrangian-Eulerian Finite Element Formulation for Incompressible Viscous Flows. *Comp. Methods Appl. Mech. Engrg.*, **29**, 329 – 349, 1981.
- [39] Johnson, C.; Nävert, U.; Pitkäranta, J.: Finite element methods for linear hyperbolic problems. *Comp. Methods Appl. Mech. Engrg.*, **45**, 285 – 312, 1984.
- [40] Kelly, D.W.; Nakazawa, S.; Zienkiewicz, O.C.: A note on upwinding and anisotropic balancing dissipation in finite element approximations to convective diffusion problems. *Internat. J. Numer. Methods Engrg.*, **15**, 1705 – 1711, 1980.
- [41] Koshizuka, S.; Nobe, A.; Oka, Y.: Numerical analysis of breaking waves using moving particle semi-implicit method. *Int. J. Numer. Methods Fluids*, **26**, 751 – 769, 1998.
- [42] Kuhnert, J.: An upwind finite pointset method (FPM) for compressible Euler and Navier-Stokes equations. In *Meshfree Methods for Partial Differential Equations*. (Griebel, M.; Schweitzer, M.A., Eds.), Vol. 26, Springer Verlag, Berlin, 2002.
- [43] Lancaster, P.; Salkauskas, K.: Surfaces Generated by Moving Least Squares Methods. *Math. Comput.*, **37**, 141 – 158, 1981.
- [44] Li, S.; Liu, W.K.: Reproducing Kernel Hierarchical Partition of Unity, Part II – Applications. *Internat. J. Numer. Methods Engrg.*, **45**, 289 – 317, 1999.
- [45] Liu, W.K.; Chen, Y.: Wavelet and Multiple Scale Reproducing Kernel Methods. *Int. J. Numer. Methods Fluids*, **21**, 901 – 931, 1995.

- [46] Liu, W.K.; Li, S.; Belytschko, T.: Moving Least Square Reproducing Kernel Methods (I) Methodology and Convergence. *Comp. Methods Appl. Mech. Engrg.*, **143**, 113 – 154, 1997.
- [47] Mittal, S.: On the performance of high aspect ratio elements for incompressible flows. *Comp. Methods Appl. Mech. Engrg.*, **188**, 269 – 287, 2000.
- [48] Monaghan, J.J.: Why particle methods work. *SIAM J. Sci. Comput.*, **3**, 422 – 433, 1982.
- [49] Monaghan, J.J.: An introduction to SPH. *Comput. Phys. Comm.*, **48**, 89 – 96, 1988.
- [50] Nävert, U.: *Finite element methods for convection-diffusion problems*. Dissertation, Dep. of Computer Science, Chalmers University of Technology, Göteborg, Sweden, 1982.
- [51] Oñate, E.; Idelsohn, S.; Zienkiewicz, O.C.; Taylor, R.L.: A Finite Point Method in Computational Mechanics. Applications to Convective Transport and Fluid Flow. *Internat. J. Numer. Methods Engrg.*, **39**, 3839 – 3866, 1996.
- [52] Oñate, E.; Idelsohn, S.; Zienkiewicz, O.C.; Taylor, R.L.; Sacco, C.: A Stabilized Finite Point Method for Analysis of Fluid Mechanics Problems. *Comp. Methods Appl. Mech. Engrg.*, **139**, 315 – 346, 1996.
- [53] Shakib, F.; Hughes, T.J.R.; Johan, Z.: A new finite element formulation for computational fluid dynamics: X. The compressible Euler and Navier-Stokes equations. *Comp. Methods Appl. Mech. Engrg.*, **89**, 141 – 219, 1991.
- [54] Tezduyar, T.E.: Stabilized Finite Element Formulations for Incompressible Flow Computations. In *Advances in Applied Mechanics*. (Hutchinson, J.W.; Wu, T.Y., Eds.), Vol. 28, Academic Press, New York, NY, 1992.
- [55] Tezduyar, T.E.; Mittal, S.; Ray, S.E.; Shih, R.: Incompressible flow computations with stabilized bilinear and linear equal-order-interpolation velocity-pressure elements. *Comp. Methods Appl. Mech. Engrg.*, **95**, 221 – 242, 1992.
- [56] Tezduyar, T.E.; Osawa, Y.: Finite element stabilization parameters computed from element matrices and vectors. *Comp. Methods Appl. Mech. Engrg.*, **190**, 411 – 430, 2000.
- [57] Tiwari, S.; Kuhnert, J.: Finite pointset method based on the projection method for simulations of the incompressible Navier-Stokes equations. In *Meshfree Methods for Partial Differential Equations*. (Griebel, M.; Schweitzer, M.A., Eds.), Vol. 26, Springer Verlag, Berlin, 2002.
- [58] Zienkiewicz, O.C.; Taylor, R.L.: *The Finite Element Method: Fluid Dynamics*, Vol. 3. Butterworth-Heinemann, Oxford, 2000.

2000-08	T. Gehrke, U. Goltz	High-Level Sequence Charts with Data Manipulation
2000-09	T. Firley	Regular languages as states for an abstract automaton
2001-01	K. Diethers	Tool-Based Analysis of Timed Sequence Diagrams
2002-01	R. van Glabbeek, U. Goltz	Well-behaved Flow Event Structures for Parallel Composition and Action Refinement
2002-02	J. Weimar	Translations of Cellular Automata for Efficient Simulation
2002-03	H. G. Matthies, M. Meyer	Nonlinear Galerkin Methods for the Model Reduction of Nonlinear Dynamical Systems
2002-04	H. G. Matthies, J. Steindorf	Partitioned Strong Coupling Algorithms for Fluid-Structure-Interaction
2002-05	H. G. Matthies, J. Steindorf	Partitioned but Strongly Coupled Iteration Schemes for Nonlinear Fluid-Structure Interaction
2002-06	H. G. Matthies, J. Steindorf	Strong Coupling Methods
2002-07	H. Firley, U. Goltz	Property Preserving Abstraction for Software Verification
2003-01	M. Meyer, H. G. Matthies	Efficient Model Reduction in Non-linear Dynamics Using the Karhunen-Loève Expansion and Dual-Weighted-Residual Methods
2003-02	C. Täubner	Modellierung des Ethylen-Pathways mit UML-Statecharts
2003-03	T.-P. Fries, H. G. Matthies	Classification and Overview of Meshfree Methods
2003-04	A. Keese, H. G. Matthies	Fragen der numerischen Integration bei stochastischen finiten Elementen für nichtlineare Probleme
2003-05	A. Keese, H. G. Matthies	Numerical Methods and Smolyak Quadrature for Nonlinear Stochastic Partial Differential Equations
2003-06	A. Keese	A Review of Recent Developments in the Numerical Solution of Stochastic Partial Differential Equations (Stochastic Finite Elements)
2003-07	M. Meyer, H. G. Matthies	State-Space Representation of Instationary Two-Dimensional Airfoil Aerodynamics
2003-08	H. G. Matthies, A. Keese	Galerkin Methods for Linear and Nonlinear Elliptic Stochastic Partial Differential Equations
2003-09	A. Keese, H. G. Matthies	Parallel Computation of Stochastic Groundwater Flow
2003-10	M. Mutz, M. Huhn	Automated Statechart Analysis for User-defined Design Rules
2004-01	T.-P. Fries, H. G. Matthies	A Review of Petrov-Galerkin Stabilization Approaches and an Extension to Meshfree Methods
2004-02	B. Mathiak, S. Eckstein	Automatische Lernverfahren zur Analyse von biomedizinischer Literatur
2005-01	T. Klein, B. Rumpe, B. Schätz (Herausgeber)	Tagungsband des Dagstuhl-Workshop MBEES: Modellbasierte Entwicklung eingebetteter Systeme
2005-02	T.-P. Fries, H. G. Matthies	A Stabilized and Coupled Meshfree/Meshbased Method for the Incompressible Navier-Stokes Equations — Part I: Stabilization
2005-03	T.-P. Fries, H. G. Matthies	A Stabilized and Coupled Meshfree/Meshbased Method for the Incompressible Navier-Stokes Equations — Part II: Coupling